Homoclinic Bifurcation as a Mechanism of Chaotic Phase Synchronization

Postnov, D.E.; Balanov, A.G.; Janson, N.B.; Mosekilde, Erik

Published in:
Physical Review Letters

Link to article, DOI:
10.1103/PhysRevLett.83.1942

Publication date:
1999

Document Version
Publisher's PDF, also known as Version of record

Homoclinic Bifurcation as a Mechanism of Chaotic Phase Synchronization

D. E. Postnov,[1] A. G. Balanov,[1] N. B. Janson,[1] and E. Mosekilde[2]
[1]*Physics Department, Saratov State University, Astrakhanskaya 83, Saratov, 410026, Russia*
[2]*Department of Physics, The Technical University of Denmark, 2800 Lyngby, Denmark*
(Received 4 August 1998)

This paper demonstrates a mechanism of chaotic phase synchronization in which the transition from asynchronous to synchronous chaos is associated with the collision of the asynchronous chaotic attractor with an unstable periodic orbit. This gives rise to a hysteretic transition with the two chaotic regimes coexisting over a certain parameter interval.

PACS numbers: 05.45.Xt

The study of coupled nonlinear oscillators is a fundamental problem in theoretical physics with applications to many areas of science and technology. Forced Van der Pol type oscillators [1] have traditionally served as a paradigm for the synchronization process, and they have provided the typical picture of the involved mechanisms. Recently, the extension of this problem to interacting chaotic oscillators has disclosed a phenomenologically similar behavior which is referred to as phase synchronization of chaos [2,3].

It has long been known that, besides local bifurcations on the surface of the resonant torus, nonlocal (or global) bifurcations also form part of the bifurcation picture in the vicinity of the synchronization region [4]. Kevrekidis *et al.* [5], for instance, have shown that the combination of local and global bifurcations is typical for chemical reaction-diffusion systems that are forced across a Hopf bifurcation. Similar results were obtained by Sturis *et al.* [6] in an investigation of insulin secretion. Knudsen *et al.* [7] have proved the existence of homoclinic bifurcation curves emanating from the points in which the torus bifurcation curves attach to the saddle-node curves of the synchronization tongues (the so-called Takens-Bogdanov points [8]).

In this Letter we show that there are systems for which the homoclinic bifurcation curves extend right down to very small but probably finite modulation amplitudes. For that kind of system, the above-mentioned mechanism of synchronization becomes the most typical one over all reasonable ranges of external forcing strength. Then, we first show that a similar homoclinic bifurcation underlies a new mechanism of chaotic phase synchronization.

The phenomena similar to that which we are going to discuss should be typical for a wide class of systems which can display homoclinic bifurcation without forcing (neuron models, reaction-diffusion systems, etc.).

However, we demonstrate that the homoclinic mechanism of synchronization can appear to be the major one in a model exhibiting homoclinic bifurcation, the latter being provided by external forcing. The model we consider naturally derives from a microbiological predator-prey problem involving interacting populations of bacteria and viruses in a continuously stirred tank reactor (chemostat).

The model reads

$$\begin{aligned}
\frac{dB}{dt} &= \nu BS\,\frac{1}{S+K} - B(\rho - \alpha\omega P)\,,\\
\frac{dI}{dt} &= \alpha\omega BP - \rho I - I/\tau\,,\\
\frac{dP}{dt} &= -P[\rho + \alpha(B+I)] + \beta I/\tau\,,\\
\frac{dS}{dt} &= \rho[F(t) - S] - \gamma\nu BS\,\frac{1}{S+K}\,.
\end{aligned} \tag{1}$$

Here, B, I, and P are the concentrations of noninfected bacteria, infected bacteria, and viruses, respectively. S represents the current concentration of nutrients inside the chemostat. Growth of the bacterial concentration B is determined by the nutrition supplement through the Monod term $\nu BS/(S+K)$, where ν is the bacterial growth rate with unlimited resources, and K is the nutrient concentration at which the growth rate is equal to half of its maximum value. γ measures the average resource consumption per bacterial cell division. Existing viruses randomly meet bacteria with collision probability α and infect them with probability ω. Infected bacteria burst after time τ releasing β new viruses. The dilution rate ρ plays the role of dissipation parameter. For large values of ρ the model displays a stable equilibrium point. As the dilution rate is reduced, self-sustained oscillations arise in a supercritical Hopf bifurcation.

Various aspects of the model have previously been studied by Baier *et al.* [9]. In the present Letter, we consider the coupling of bacteria-virus populations via the flow of nutrients along a chain of chemostats. This implies that the inlet concentration of nutrients to a given chemostat will depend on the overflow from the preceding chemostat. In this way, each pool will be forced with a signal that depends on the dynamics of the upstream pool. Throughout the study, we have used the same parameters as used by Baier *et al.* [9]. Values of the nutrient inlet concentrations σ_i will be given in μg/ml, and values of the bacteria and virus concentrations in $10^6/\mathrm{ml}^{-1}$.

 0031-9007/99/83(10)/1942(4)$15.00

Let us first consider the periodically forced model (1), i.e., the system for which $F(t)$ simulates the activity of a single oscillating bacteria-virus population upstream to our chemostat. To do so, we express the incoming resource flow as a time periodic function:

$$F(t) = \sigma\left[1 - \frac{m}{2}(1 - \sin(\Omega t)\right], \qquad (2)$$

where Ω represents the modulation frequency while m is the modulation depth. In the notation of (2) σ denotes the maximal resource concentration. Figure 1 displays part of the parameter plane near the main 1:1 resonance. Here, the curves SN are saddle-node bifurcation curves, H are curves of homoclinic bifurcations, and T is a torus bifurcation curve.

In the regions immediately outside the saddle-node bifurcation curves, the system displays a single quasiperiodic attractor. This is illustrated in Fig. 2a. At the saddle-node bifurcation curves, a pair of periodic orbits, one stable and the other unstable, are born outside the torus. As shown in Fig. 2b the unstable manifolds of the saddle cycle connect to the stable cycle on one side and approach the torus on the other. The stable manifold of the saddle cycle (not shown) divides the basins of attraction for the two asymptotic solutions. Along the homoclinic bifurcation curves, the torus makes contact with the saddle cycle [10] and disappears in a boundary crisis (Fig. 2c), and between the two homoclinic bifurcations the system displays a stable and an unstable periodic orbits in a heteroclinic structure that is topologically equivalent to a resonant torus.

Thus, there are two different tori involved in the process, and the transition between them is accomplished via the homoclinic bifurcation. In previous studies this type of transition was observed only for a rather limited region of relatively strong coupling [4–6]. By contrast, we have found a tangentlike location of the SN and H curves. We suppose that the reason for this phenomenon might be the specific features of the autonomous model (1), namely, the limit cycle trajectory goes very close to stable and unstable manifolds of the saddle point at origin. However, precise explanation requires new serious investigations which we plan for the future.

Returning now to the behavior of an array of coupled population pools, we first note that the case of two coupled bacteria-virus populations is equivalent to the nonautonomous case and displays the same kind of behavior. Next we consider a system of three coupled bacteria-virus populations. If we define the inlet concentrations $F_{1,2,3}(t)$ as

$$F_1(t) = \sigma_1; \qquad F_2(t) = S_1 + \sigma_2; \qquad F_3(t) = S_2 + \sigma_3, \qquad (3)$$

where the subscript denotes the pool number, the forcing parameters for the second and third pools are produced in accordance with the predator-prey dynamics of the upstream pool.

With $\sigma_2 = 0$, by the choice of σ_1 we can vary the type of forcing signal applied to the third population from regular to chaotic oscillations, and by using an appropriate value of σ_3 we can observe either a synchronous or an asynchronous response of the third system to the forcing signal.

The main regimes observed and the corresponding bifurcation curves are displayed in Fig. 3. For $\sigma_1 < 12.48$, the nutrient concentration in the outflow from the second chemostat follows a simple limit cycle oscillation, and variation of σ_3 towards the left-hand part of the diagram (not shown) realizes the homoclinic synchronization mechanism as described for the nonautonomous bacteria-virus population.

The right border (T_1 line) is the torus bifurcation line. However, no stable torus appears at this line, only the loss of stability for the periodic solution near the saddle cycle. As it was proved for the two-dimensional system, this kind of transition is accompanied by a global bifurcation involving the homoclinic orbit of the saddle [11]. Higher values of σ_1 allow us to observe qualitatively the same

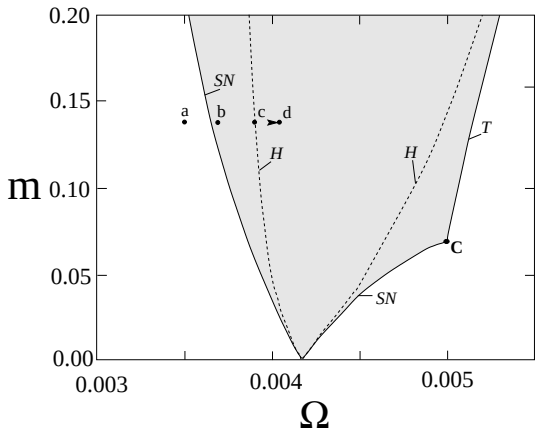

FIG. 1. Part of the bifurcation diagram for the nonautonomous bacteria-virus population. C indicates a Takens-Bogdanov point.

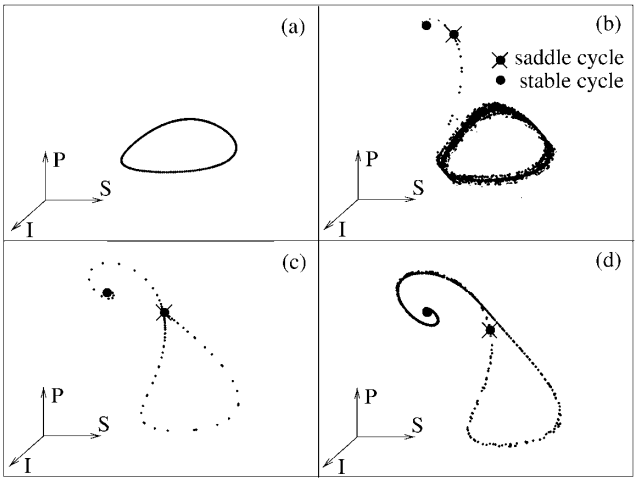

FIG. 2. Poincaré sections illustrating the structural changes that occur along the point sequence a, b, c, and d in Fig. 1.

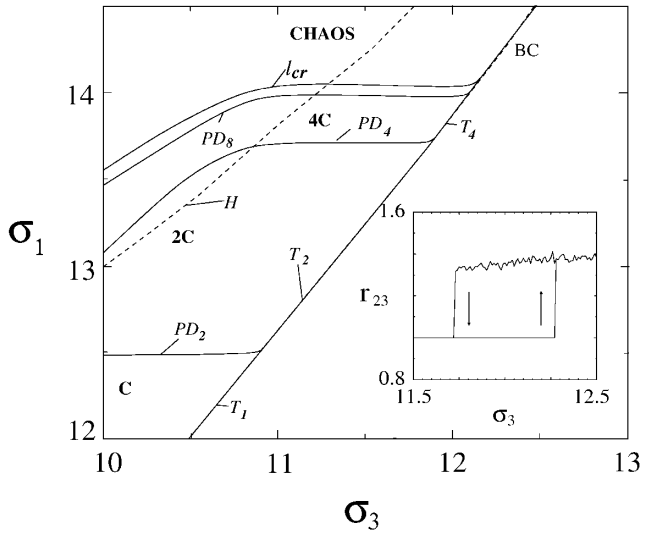

FIG. 3. Bifurcation diagram for the system of three bacteria-virus populations. The inset shows the variation of r_{23} vs σ_3.

phenomena for the period-2 and period-4 limit cycles. Finally, when σ_1 exceeds 14.07 we observe a hysteresis behavior and a crisislike transition between two chaotic attractors.

To classify these attractors and the crisis itself, let us recall some results on phase synchronization of chaos [2,3]. For periodically forced chaotic systems it has been found that there are two main types of chaotic attractors. The first is qualitatively equivalent to the period-doubling chaos of the autonomous chaotic system with a fundamental frequency governed by the frequency of the external signal. Following [2] let us term this chaotic regime as "synchronous chaos." The second type of chaotic attractors is torus chaos with a power spectrum that exhibits two fundamental frequencies above the continuous background. By analogy with the quasiperiodic (asynchronous) nonchaotic behavior let us term this regime as "asynchronous chaos."

Besides by the specific form of their phase projections, Poincaré sections, and power spectra, the two types of behaviors can be easily distinguished by following the phase of the chaotic attractors [3,12] or by calculating their *mean return time to a Poincaré secant* [13].

We have used the mean return time to classify the different chaotic regimes of our model. We fixed the resource concentration in the first chemostat at $\sigma_1 = 14.25$ and defined the Poincaré secant for each subsystem as

$$B_i = P_i/5, \qquad i = 1 \ldots 3. \tag{4}$$

The mean return times were hereafter calculated for the three subspaces (B_i, I_i, P_i, S_i), $i = 1 \ldots 3$. The ratios between the mean return times provide the two winding numbers r_{12} and r_{23}. The value of r_{12} was found to be 1.0000 ± 0.0001 at any point of the diagram in Fig. 3. This is consistent with the fact that the choice of $\sigma_2 = 0$ in the second chemostat produces synchronous (chaotic or regular) regimes only.

The variation of r_{23} versus σ_3 is depicted in the inset of Fig. 3. One can see the two overlapping branches. One of them falls directly at $r_{23} = 1.000 \pm 0.001$ while the other shifts slightly with σ_3, assuming a range of values between 1.3 and 1.4.

Together with other observations the above result clearly shows that the considered chaotic attractors represent synchronous (branch $r_{23} = 1.0$) and asynchronous chaos in the sense of Refs. [2,3,14]. However, the transition between the two chaotic attractors is of a different type. In the above-mentioned works the coexistence of synchronous and asynchronous chaotic regimes was not found, and the whole picture of transition between these regimes differed significantly from that observed here. In our case the transition is consistent with the *homoclinic synchronization mechanism* we already illustrated for the regular oscillations.

To support this conclusion, the Poincaré section was calculated at the center of the coexistence area and at the homoclinic bifurcation curve H. The results are shown in Fig. 4. One clearly sees that the asynchronous chaos touches the unstable cycle at the point of crisis $\sigma_3 = 11.73$.

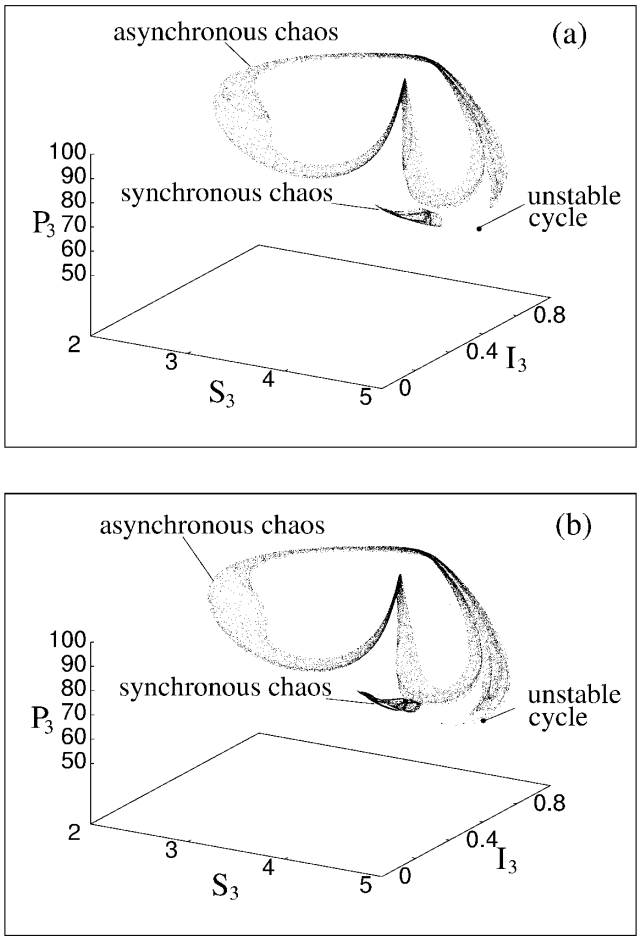

FIG. 4. Poincaré sections of the two coexisting chaotic attractors for $\sigma_3 = 12.25$ (a) and $\sigma_3 = 11.73$ (b). $\sigma_1 = 14.25$, $\sigma_2 = 0$.

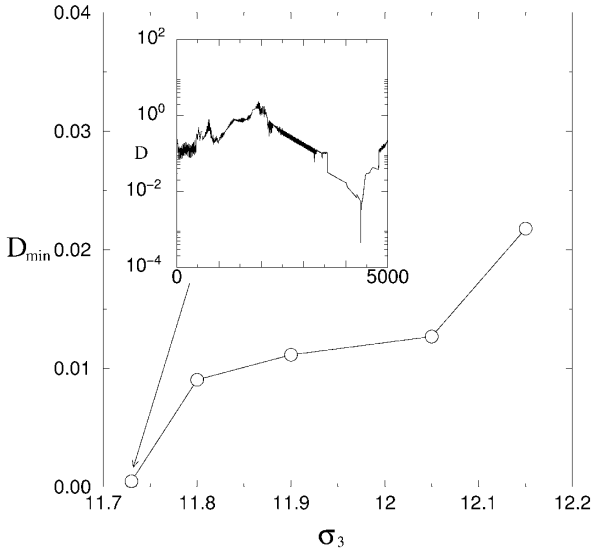

FIG. 5. Minimal distance between the saddle cycle and the asynchronous chaotic attractor for $\sigma_1 = 14.25$. The inset shows the distance profile along the saddle cycle at $\sigma_3 = 11.73$.

Of course, for such a high-dimensional system such as our coupled bacteria-virus model, it is difficult to make precise statements about the mutual configuration of attractors basing on Poincaré sections only. However, useful information can be obtained by calculating the distance between the specified objects in phase space. In Fig. 5 the variation of the minimal distance between the asynchronous chaos and the saddle cycle is plotted as a function of the parameter σ_3. In the inset the distance profile along the saddle cycle at $\sigma_3 = 11.73$ is shown. 5000 points were recorded along the saddle cycle. The minimal distance is shown for each point. The tangency of attractors is about to occur at the point number 4367. As one can see, the chaotic attractor really approaches the saddle cycle and touches it at the point of bifurcation $\sigma_3 \approx 11.73$.

In conclusion, we have demonstrated the example of dynamical system for which synchronization via the homoclinic bifurcation appears to be the major synchronization mechanism. It has been shown that the above mechanism remains valid even in the case of chaotic forcing. The latter result represents a novel mechanism of phase synchronization of chaos.

This work is supported in part by the Russian State Committee of Science, INTAS (INTAS Grant No. 96-0305) and RFFI (Grant No. 98-02-16531). D. P., A. B., and N. J. acknowledge support from the Danish Research Academy.

[1] See, e.g., C. Hayashi, *Nonlinear Oscillations in Physical Systems* (McGraw-Hill, New York, 1964).
[2] V. S. Anishchenko, T. E. Vadivasova, D. E. Postnov, and M. A. Safonova, Int. J. Bifurcation Chaos Appl. Sci. Eng. **2**, 633 (1992); V. S Anishchenko, T. E. Vadivasova, D. E. Postnov, O. V. Sosnovtseva, L. O. Chua, and C. W. Wu, Int. J. Bifurcation Chaos Appl. Sci. Eng. **5**, 1525 (1995).
[3] M. G. Rosenblum, A. S. Pikovsky, and J. Kurths, Phys. Rev. Lett. **76**, 1804 (1996); A. S. Pikovsky, M. G. Rosenblum, and J. Kurths, Europhys. Lett. **34**, 165 (1996); G. V. Osipov, A. S. Pikovsky, M. G. Rosenblum, and J. Kurths, Phys. Rev. E **55**, 2353 (1997).
[4] J. Guckenheimer and P. Holmes, *Nonlinear Oscillations, Dynamical Systems, and Bifurcations of Vector Fields* (Springer-Verlag, New York, 1986), p. 459.
[5] I. G. Kevrekidis, R. Aris, and L. D. Schmidt, Physica (Amsterdam) **23D**, 391 (1986); M. A. Taylor and I. G. Kevrekidis, Physica (Amsterdam) **51D**, 274 (1991).
[6] J. Sturis, C. Knudsen, N. M. O'Meara, J. S. Thomsen, E. Mosekilde, E. Van Cauter, and K. S. Polonsky, Chaos **5**, 193 (1995).
[7] C. Knudsen, J. Sturis, and J. Skovhus Thomsen, Phys. Rev. A **44**, 3503 (1991).
[8] R. I. Bogdanov, Funct. Anal. Appl. **9**, 144 (1975).
[9] G. Baier, J. S. Thomsen, and E. Mosekilde, J. Theor. Biol. **163**, 593 (1993).
[10] More precisely, when the torus approaches the saddle cycle, the rather local folding occurs. That process does not involve the manifolds of saddle cycle but destroys the torus via the "loss of smoothness" right before the homoclinic event while most of the torus surface remains smooth.
[11] V. I. Arnold, in *Nonlinear Waves*, edited by A. V. Gaponov-Grechov (Nauka, Moscow, 1979); K. Kaneko, *Collapse of Tori and Genesis of Chaos in Dissipative Systems* (World Scientific, Singapore, 1986).
[12] E. Rosa, E. Ott, and M. H. Hess, Phys. Rev. Lett. **80**, 1642 (1998).
[13] A. B. Neiman, Phys. Rev. E **49**, 3484 (1994).
[14] T. Yalcinkaya and Y. C. Lai, Phys. Rev. Lett. **79**, 3885 (1997).